Development of a Multi-Energy Flash Computed Tomography Diagnostic for Three Dimensional Imaging of Ballistic Experiments

Michael B. Zellner[1, a)], Kyle Champley[2], Larry McMichael[2], Harry Martz[2], Ronald Cantrell[3], Corey E. Yonce[3], Kenneth W. Dudeck[1], Chester A. Benjamin[1], Robert W. Borys[3], David R. Schall[1], Allen P Ducote III[1], Thomas J. O'Connor[3], Thomas E. Nellenbach[3], Nathan J. Sturgill[3], Thomas L. Quigg[3], Seth T. Halsey[1], Jennifer A. Benjamin[3], and Benjamin P. Huntzinger[3]

[1]*U.S. Army Research Laboratory*
321 Colleran Rd
Aberdeen Proving Ground, MD 21005.
[2]*Lawrence Livermore National Laboratory*
7000 East Ave.
Livermore, CA 94550-9234.
[3]*Bowhead Science and Technology*
103 Beta Blvd.
Belcamp, MD 21017.

[a)]michael.b.zellner.civ@mail.mil

Abstract. The U.S. Army Research Laboratory, in conjunction with Lawrence Livermore National Laboratory, is developing a Multi-Energy Flash Computed Tomography (MEFCT) diagnostic that will be used to capture tomographic image(s) of dynamic impact and detonation events. To accomplish dynamic tomography, the diagnostic uses numerous source–detector pairs to accumulate up to fifteen two-dimensional images, which are subsequently used to compute up to three three-dimensional tomographic reconstructions. The diagnostic is designed to provide either: a single-frame, three-dimensional tomographic reconstruction that delineates material specificity throughout the field, or a three-frame tomographic reconstruction movie spaced in time, while lacking the information pertaining to the material specificity. This work assesses aspects of the diagnostic development including structural design, dynamic capability, instrument resolution and computational reconstruction. Examples of real-time measurements are provided from static phantom fiducials, as well as a dynamic experiment depicting a non-symmetric ballistic penetration to demonstrate the usefulness of the capability.

INTRODUCTION

The U.S. Army has a need to understand dynamic material response at scales representative of actual penetrator/target configurations. However, understanding this response in a predictive capacity is prohibitive because the classical global motions and responses are governed by the superposition of many subatomic entities that respond in a chain-reaction process. In an attempt to gain a fuller understanding of the material response for predictive applications, scientists observe material interactions at some level and hypothesize theories that describe phenomena such as fracture, chemical reactions, and electrical conduction. These hypotheses are often limited by the resolutions and techniques that scientists can use to probe the interactions *in situ*, but ultimately feed the theories and models developed to describe such global responses. The need to observe material response at increasing fidelity and

dimensionality drives the evolution of diagnostic capabilities to probe large quantities of interactions across a vast range of length-scales.

This report describes the development of an improved radiographic computed tomographic technique that has the potential to identify materials within a three-dimensional spatial field, at the sub millimeter resolution, on ballistic timescales [1]. Although this spatial resolution is subpar compared to current optical-based photographic techniques, computed radiography in general benefits from use of X-rays with energies spanning 1 – 1000 KeV. This energy spectrum is more penetrating than that of conventional photography, as the X-ray photons interact with materials via different scattering mechanisms. Computed tomography therefor allows scientists to image internal material structures, which are typically obscured by surface scattering and optical blinding that can occur with more conventional photographic techniques. In medical fields, use of X-rays computed tomography has contributed to visualizing bone, tissue, and organ structures below the epidermal layer. When combined with reduced timescales as in the current work, this will allow for identification of material responses interior to their surface under dynamic response. This could be how a piston reacts during deflagration of fuel inside an engine cylinder or how a cavity forms as a bullet penetrates a target. This diagnostic is an extension of work performed by Moser et al. [2] in which multiple flash x-radiograph source/detector pairs was used to acquire data that was subsequently combined using novel iterative computed tomography techniques to produce a single three-dimensional attenuation volume-space. The current work expands on this technique by incorporating multiple discrete energy sources into the technique. In addition to generating more images throughout the event, this will allow users to take advantage of the known variation in spectral attenuation response of materials, which will allow for discernment of material specificity similar to that of conventional (long timescale) X-ray computed tomography [3]. Because of the short acquisition timescales, the potential to resolve multiple materials, and the ability to resolve the materials in three spatial dimensions, this diagnostic may demonstrate usefulness in any field that involves dynamic material response phenomena such as material mixing, material flow, material fracture, material densification, etc.

HARDWARE DESIGN AND CONSIDERATIONS

Design of the MEFCT diagnostic was based on two self-imposed requirements: 1) the ability to capture three consecutive three-dimensional images throughout the evolution of a dynamic event, and 2) the ability to discern three materials plus void at a single point in time of a dynamic event. Theoretically, one can compute a single tomographic reconstruction if three orthogonal two-dimensional radiographs of high quality are acquired. Therefore, three sets of three flash-discharge source-detector pairs capable of viewing the dynamic event would be required to meet the base requirements. In practice, however, it is difficult to acquire two-dimensional projections of sufficiently high quality during a ballistic-timescale dynamic event, as the flash-discharge sources and detection methods are limited in their capability with respect to sufficient signal-to-noise ratio and consistency of signal dynamic range. These limitations can be overcome by including additional projections from off-axis perspectives. Taking into consideration (1) the ability to physically accommodate multiple sources and detectors in a spherical volume, (2) the size of the completely sampled and partially sampled X-ray field-of-view, (3) the signal-to-noise and uniformity of the resulting two-dimensional projections, (4) Compton scattering effects, (5) software and current iterative reconstruction techniques, and (6) cost, it was decided to construct a device that used five two-dimensional projections to create each tomographic reconstruction.

The general arrangement of the 15 flash-discharge sources and detectors is shown in FIGURE 1. In the photograph, sources are painted blue and the detectors take the form of large grey rectangles connected using aluminum members. The source/detector pairs are affixed opposite each other on a set of three interlaced rings, the largest of which is 2.6 m in diameter. In a typical test, the target is suspended in the center of the sphere. The rings can rotate along the vertical axis in FIGURE 1, allowing for flexibility of experiment parameters (viewing angles, flying fragments, loading drivers, etc.). For dynamic tests that result in blast-loading of the structure, the detectors can be mounted using nylon shear tabs that allow the detectors to fly free thus minimizing loading of the aluminum spherical structure. This technique has been tested for blast loadings up to 1.5 lbs TNT equivalent when detonated at the center of the sphere [4]. In all dynamic testing it is necessary to encase the imaging plates to protect them from fragment and blast loading.

To identify material type, the MEFCT technique plans to take advantage of the variance in scattering cross section as a function of material and photon energy. This variance is depicted in FIGURE 2, which shows the total X-ray attenuation coefficient (sum of all interaction cross sections) as recorded by National Institute of Standards and Technology (NIST) for multiple materials of interest [5]. Utilization of broadband flash-discharge X-ray sources of

varying peak energies will allow for a decomposition routine to identify materials based on attenuation comparisons if all three of the tomograms are computed at the same time during the dynamic event.

The individual two-dimensional projections are generated using L3 Applied Technologies flash-discharge X-ray sources. The sources generate a broadband spectrum of X-rays, characterized by a total radiation dose of approximately 80 mrem at a distance of 150 mm during a 60-80 ns pulse. This is accomplished by discharging a high-voltage Marx bank capacitor across a tungsten anode vacuum tube. These X-rays are incident on the material of interest during a dynamically driven event, and the ones that are not scattered are collected by Carestream IRC2 digital imaging plates located on the opposite side of the event. The digital imaging plates utilize a phosphor material that absorbs within the X-ray energy region to trap electrons into an excited state. Post-experiment, the imaging plates are inserted into a Carestream HPX-1 scanner that rasters a red laser across the digital imaging plate, which pumps the trapped electrons over an activation barrier, causing them to emit a blue photon while relaxing to a reduced state. A photodiode collects the blue photons, which are in proportionality to the non-scattered X-rays, producing the X-ray attenuation image contrast.

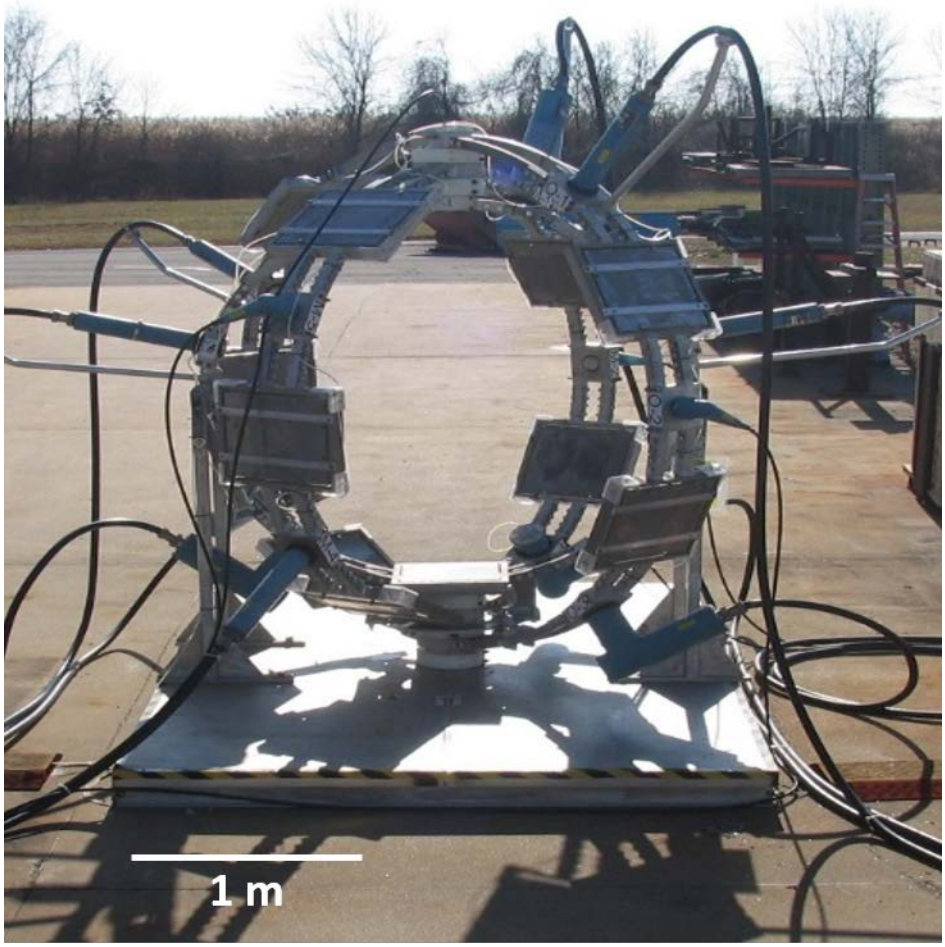

FIGURE 1: Organization of the 15 flash-discharge X-ray sources (blue tubes, five 150 KeV, five 300 KeV, and five 450 KeV) and detectors (grey rectangles) on three interlaced spheres.

The complex process of generating individual two-dimensional radiographic projections, combined with the specifications imposed by the mathematics designed to generate the three-dimensional tomographs warrants a discussion of where errors can arise throughout the process and how they affect the overall result. Unlike conventional computed tomography where a single source and detector are used to collect all two-dimensional projections in a serial manner, use of multiple sources simultaneously can result in variances in the flux and spectral distribution during generation, propagation, and detection of the X-rays.

During generation influences are realized through: (1) charging differences of the individual Marx bank capacitors that define the total energy supplied to the generation process, (2) transmission of the energy from the charging units to the capacitors, and then from the capacitors through the remote cables to the vacuum tubes within the tube heads, and (3) conversion of the stored electrical energy into X-rays within the vacuum head that contains the anode/cathode pair. To minimize charging differences, all capacitors of the same class energy sources are tied to a single high voltage supply and charged to a single operating potential (three voltage supplies in total, one each for the 150, 300, and 450 KeV classes). Because individual variances occur within the stack of capacitors that compose each Marx bank, the self-discharge and no-discharge curves were balanced using adjustment of the initiation spark gaps and pressure of the dry air pumped inside the capacitor housing. Concerning the energy transmission, it is most important to ensure impedance balance of the remote tube-head cables, and impedance of tubes. This is particularly important when driving multiple tubes with a single capacitor so that the energy is directed to the tubes and not discharged along the length of the cables. It is also important to recognize that because the energy pulses occurs over ~60-100 ns, impedance measurements must be made using 10-17 Mhz frequency which travels near the surface of conductors. When the energy is converted to X-rays, focus shifts to variations induced from changes that occur to the anode every shot as a result of heat loading/dissipation, ablation, etc. There is little influence the user has here other than to monitor the changes and replace parts when degraded.

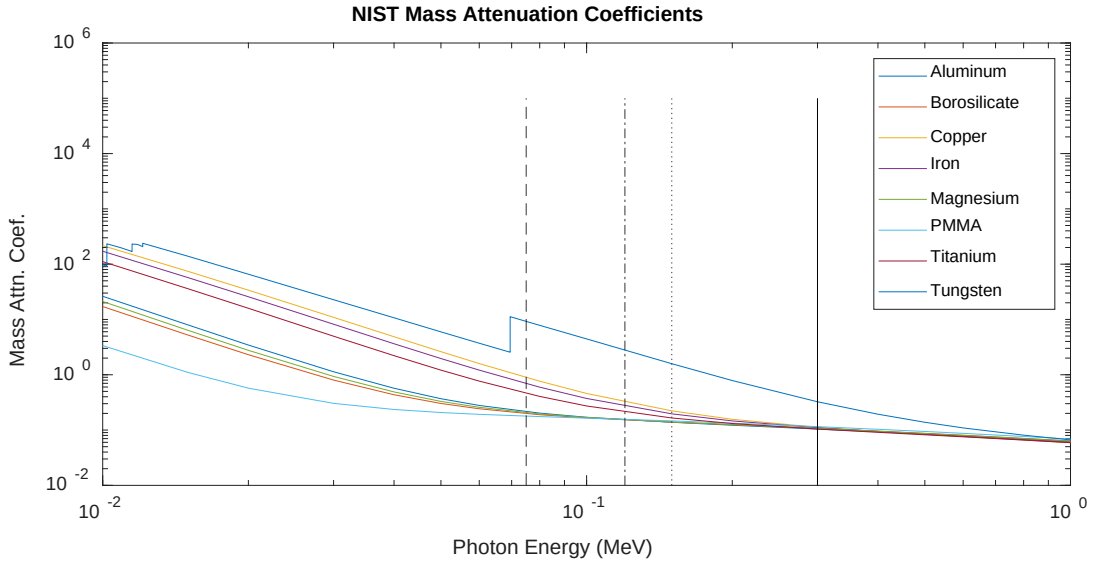

FIGURE 2: Mass attenuation coefficients for multiple materials of interest as published on the NIST database. The dashed, dash-dot, dotted, and solid black lines approximate the energy at which the peak X-ray flux is generated from the 150, 300, 450, and 1000 KeV broadband sources, respectively.

During the time from X-ray generation to X-ray detection, influences arise based on the physical scattering mechanisms of 1-450 KeV X-rays. In this this portion of the spectrum, both the Photoelectric transitions and Compton scattering contribute. In the present case, numerous sources emit X-ray photons over a wide geometry and large solid-angles, which are collected by all detectors that are "always on". Unfortunately, the X-rays cannot be focused or steered without a significant decrease in flux, so one must rely on shielding as the sole influence to minimize undesired X-rays corrupting neighboring detectors. Further, Compton scattered low-energy photons from near-surface scattering events are generated from the target and supporting structure that can corrupt neighboring detectors. Propagation influences also arise from the need to shield the detectors from blast effects. This increases the X-ray scattering potential in metal and polymer protective layers, reducing the overall signal from the event of interest.

During detection inefficiencies primarily arise from the need to be able to temporally store the radiographic information from the ~60-100 ns exposure duration until one can digitize the results. Here, insuring the digital imaging plates are not exposed to light prior to reading with the scanner, and control of the light (both excitation and collection) in the scanner are of utmost importance. Calibration of the scanner, specifically the gain on individual photodiodes within the array that raster across the digital imaging plate to collect fluoresced photons from relaxing electrons, was found to be the most effective method for balancing the readings from the individual imaging plates.

It is also important to be very precise in positioning of the detectors as they are inserted and removed from the device. This is necessary as one must compensate the dynamic images using initial irradiance (static) and dark-field images to compute the transmission attenuation, which are in turn used for computing the attenuation tomograph.

SOFTWARE INCORPORATION

The MEFCT utilizes the Livermore Tomography Tools (LTT) software suite developed by Lawrence Livermore National Laboratory to perform the tomographic reconstruction (6). LTT is a comprehensive computed tomography software suite that incorporates vast flexibility in its use of methodologies, algorithms, and input geometries from which it computes a 3-D image. The software is capable of running on Windows, Macintosh, or Unix platforms, and is capable of being run in serial or parallel hardware configurations. LTT is particularly well suited to the MEFCT diagnostic in that it is flexible with respect to input geometry using its Modular Cone Beam input. This is of great importance because the MEFCT has a non-symmetric structure to minimize X-ray corruption on neighboring source/detector pairs, while optimizing the amount of near-orthogonal off axis views of the object. Flexibility is also needed as the geometry can be altered by rotating the set of interlacing rings to accommodate experiments where blast and high-velocity fragments.

In concert with the capability of reconstructing from Modular Cone Beam input, LTT has a vast amount of iterative reconstruction numerical optimization algorithm/solvers and cost functions. To pre-process the images, LTT has numerous built-in routines including outlier removal, beam hardening correction image rotation, image cropping, scaling, debluring, etc. LTT also has implementations of dual- and triple-energy routines for material identification, but these routines require that the projection data for each spectra be registered. In future work, we will use an iterative multi-material beam hardening correction in LTT for beam hardening correction and material characterization.

FIGURE 3 shows a flow chart that describes the path LTT navigates to produce a 3-D attenuation reconstruction from the multiple 2-D projection radiographs. This path begins with input of five 16-bit tif files for each of the dynamic, static, and dark field projections, and a comma separated geometry file describing the location and orientation of the X-ray sources and detectors. These images are preprocessed for by cropping to size, corrections for outliers and generated into transmission images. The images are then corrected for low signal anomalies that can arise from noise and misalignment when computing the transmission values. The corrected transmission radiographs are then down-sampled to reduce noise and speed up the reconstruction (this step may be omitted in future analysis). The results are combined with the geometry file and processed using iterative reconstruction routines to create the 3-D attenuation tomographic reconstruction image. For a static fiducial comprising of different sized metal spheres, the computational reconstruction takes approximately an hour with most of this processing time being dominated by the iterative reconstruction step after preprocessing has been complete.

FIRST DYNAMIC EXPERIMENT

The first dynamic experiment focused on acquiring a data set that included unique three-dimensional structures, resolving timing issues, and demonstrating system capability. For demonstration purpose, a 30 caliber APM2 bullet was imaged after perforating a 10 mm thick 7039 aluminum plate. The striking velocity was 914 m/s. A photograph of the MFECT diagnostic with the gun and velocity screens is depicted in FIGURE 4. During the experiment, the target was suspended from the top of the MEFCT support structure using a nylon stand, and secured using strips of duct tape and further constrained by inertial forces as shown in FIGURE 5. Time-of-impact was recorded using a polyvinylidene fluoride (PVDF) piezoelectric film that was secured to the back of the plate. The piezoelectric signal was also used to start-trigger the MEFCT system timing and end-trigger the velocity screen oscilloscope. The MEFCT's 300 KeV set of sources were discharged 110 μs after plate impact to collect a set of radiographs of the bullet and ejected fragments. In addition, a Photron SAZ was used to photograph the event. The camera used a 2.5 μs gate and a 8.33 μs inter-frame spacing (120,000 fps). With the lens setup used, the images depict a 500 x 250 mm field-of-view mapped to a 512 x 264 pixel image. FIGURE 6 shows a frame sequence depicting the penetration event using 12 frame jumps, which corresponds to a temporal spacing of 100 μs between images. In this sequence, the third image roughly corresponds with the time at which the MFECT collected the two-dimensional projections. FIGURE 7 shows the five individual two-dimensional projection radiographs that were collected via the MEFCT diagnostic simultaneously. The images were scanned with 50 micrometer square pixel resolution, resulting in multiple 8636 x 7040 pixel radiographs. The radiographs were stored in 16-bit tiff grayscale image format, with the data residing within the lowest 250 bits. FIGURE 8 shows one perspective of the three-dimensional reconstructed attenuation

tomograph. The tomograph was reconstructed using LTT with an iterative routine. A movie of the three-dimensional attenuation rotating 360° in volume space is attached as a .MPI file and available via email of the corresponding author.

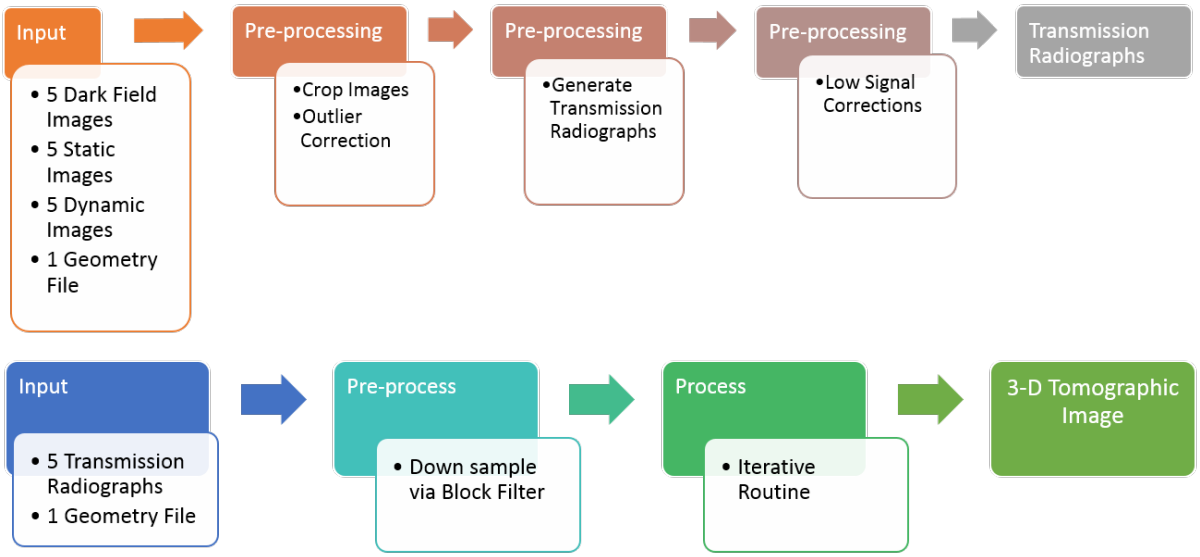

FIGURE 3: Flow chart describing the path LTT navigates to produce a three-dimensional attenuation reconstruction from the multiple two-dimensional projection radiographs. This path must be navigated for each tomographic reconstruction (i.e. the 150 KeV, 300 KeV, and 450 KeV reconstructions).

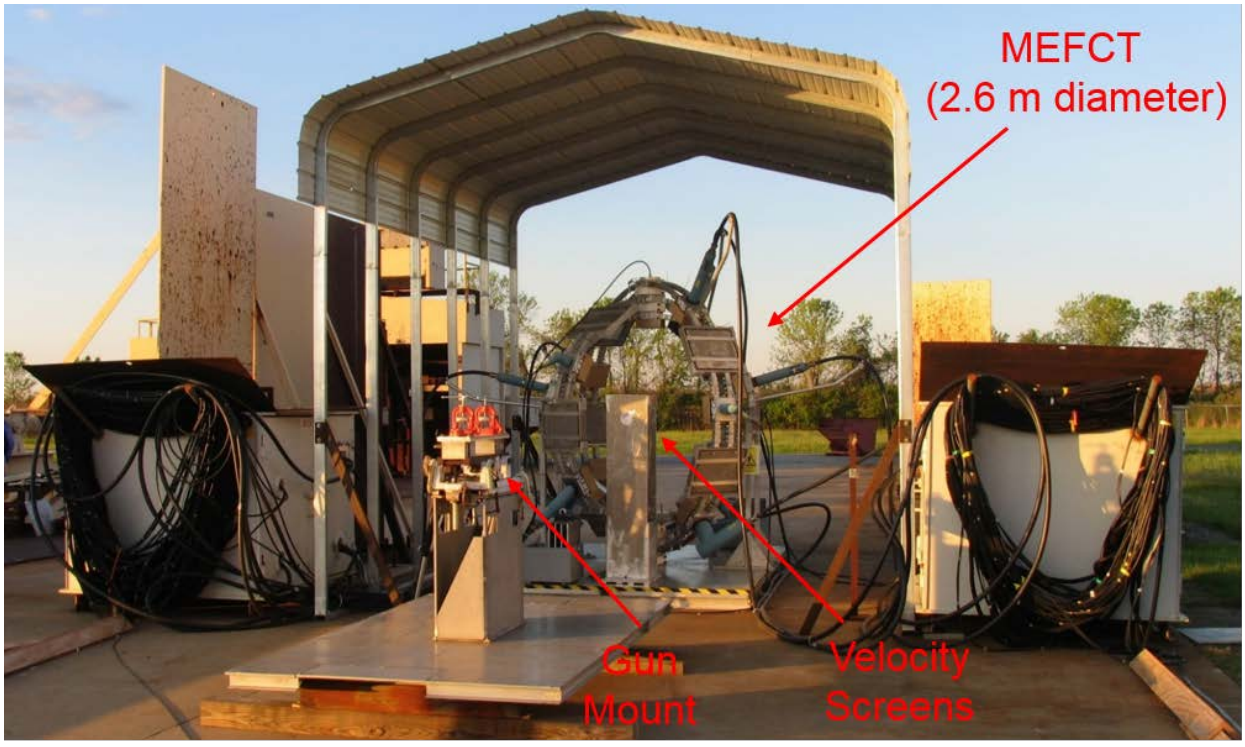

FIGURE 4: Photograph of the MEFCT diagnostic as used during the first dynamic experiment showing the gun and velocity screens.

FIGURE 5: Image depicting the first dynamic experiment's nominally 200 x 200 x 10 mm Al target and support platform.

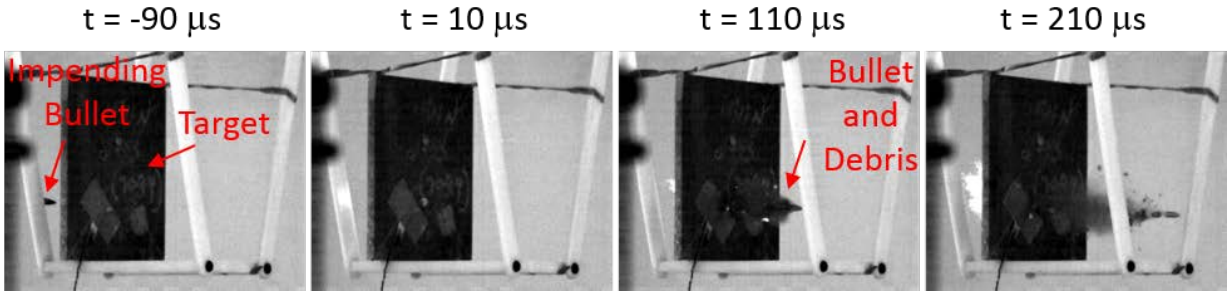

FIGURE 6: Frame sequence from the Photron SAZ that depicts the ballistic impact event of the first dynamic experiment. The third image corresponds to the time at which the MEFCT was utilized.

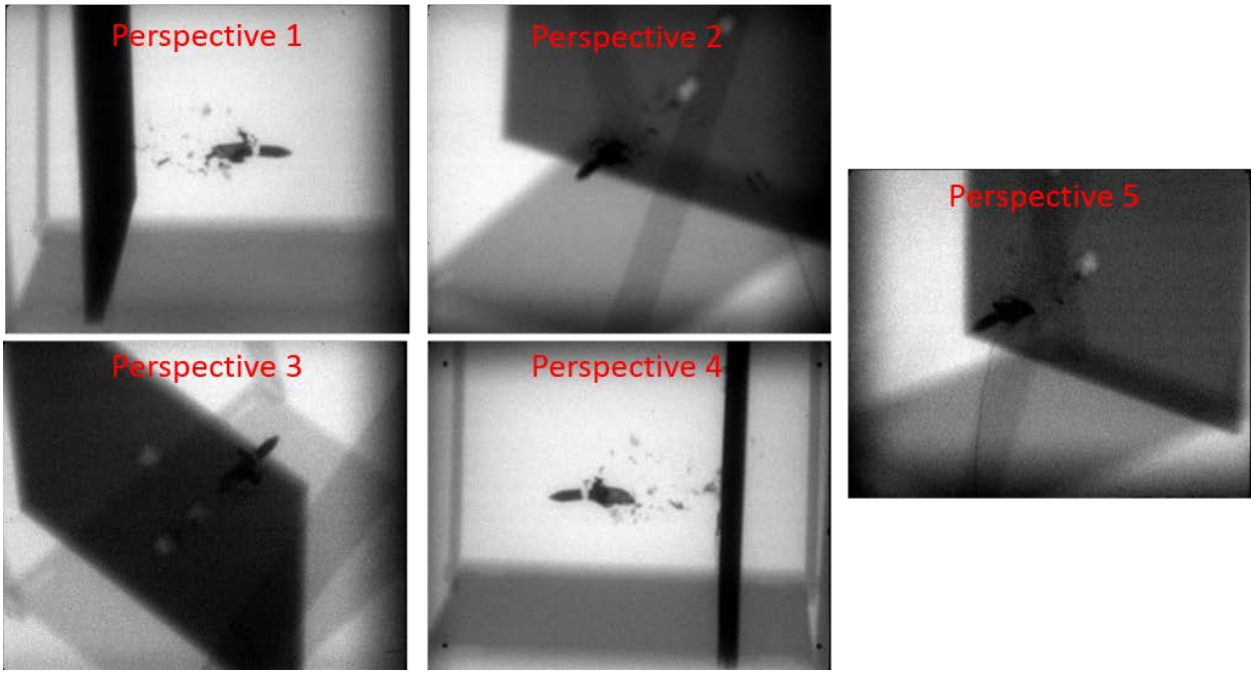

FIGURE 7: Two-dimensional X-ray projections of a bullet after exiting an Al 7039 plate from 5 different perspectives.

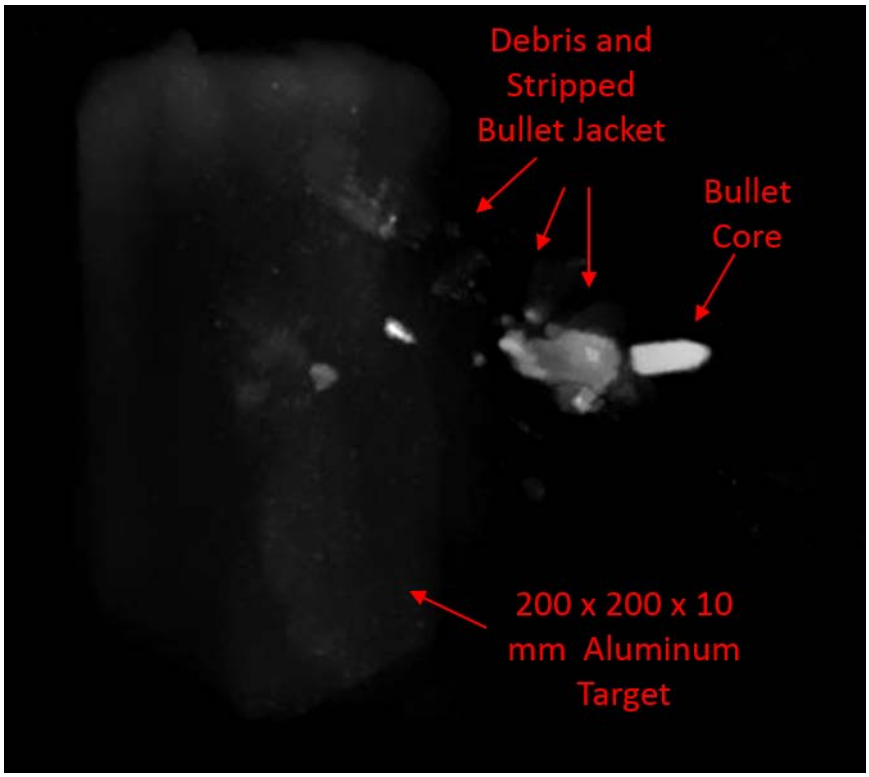

FIGURE 8: Maximum intensity projection (MIP) from the three-dimensional reconstruction of a bullet after penetrating an Al 7089 plate. For scale, the target is approximately 200 x 200 x 10 mm and the core of the bullet is approximately 27 mm long.

In the resulting reconstruction one can identify the aluminum target plate with a hole in it, a debris field, and the bullet's hardened steel core. The reconstruction was digitized over a 750 x 750 x 750 voxel space, which is of lesser resolution than the 8636 x 7040 pixel projections. The reduced subspace slightly reduced image noise, and also served to manage total computational time. In the reconstruction, the aluminum target plate is of modified attenuation values. This phenomena results from the plate residing outside of the fully-sampled volume space. To complete the volume reconstruction without artifacts, the original two-dimensional projections were bounded (cropped), which resulted in the modified field values. One could perform the reconstruction without this modification if the focus were on the plate and the penetration hole, but artifacts would be projected throughout the reconstruction volume. The bullet and the fragment field, however, reside within the fully-sampled region. In the reconstruction, it is clear that the copper jacket is stripped from the heavy core of the bullet, and that this core ejects with pitch and yaw. The dense debris cloud immediately following the core is assumed to partially comprise of the copper jacket material. One is able to step through this attenuation volume space to visualize the hollowness of the jacket. At larger radii, and extending back to the plate, multiple particle fragments are visible. Within this region, we are able to resolve particles at less than 1 mm diameter. We cannot yet discern material composition, but should have this capability when the spectral component is added to the analysis.

CONCLUSIONS AND PATH FORWARD

The U.S. Army Research Laboratory, in conjunction with Laurence Livermore National Laboratory, have constructed a multi-energy tomographic diagnostic capable of capturing three-dimensional attenuation volumes during ballistic timescale events. The diagnostic is currently capable of collecting three three-dimensional snapshots in time, and is planned to be capable of performing in a mode where it captures a single snapshot in time while being able to discern up to three types of materials and void. A dynamic experiment was conducted to assess the systems capabilities and resolution. During the dynamic experiment a bullet was imaged after penetrating an aluminum plate. A tomographic reconstruction was performed using Livermore Tomography Tools software suite. The resulting reconstruction had sub-millimeter resolution and sufficient contrast to image the target plate with a hole in it, the

bullet, its pitch and yaw, and the fragment field generated at impact. Improvements will be made to incorporate a spectral component to allow for material identification.

ACKNOWLEDGMENTS

The authors would like to thank Dr. Stephan Moser and Dr. Siegfried Nau of Ernst Mach Institute for their insightful additions to this project through conversation during the initial stages. We thank Dr. Richard Becker and Kaden Uhlig for their contributions in overall implementation of the device and development of code to allow for use under conditions when the sources/detectors undergo movement. The authors would also like to thank members of the ARL Welding and Carpenter shop for their efforts to design and construct the MEFCT device and supporting structures.

The Livermore Tomography Tools software package was written by Kyle Champley, Trevor Willey, Hyojin Kim, and Karina Bond.

The research reported in this document/presentation was performed in connection with contract/instrument W911QX-17-C-0021 with the U.S. Army Research Laboratory. The views and conclusions contained in this document/presentation are those of the authors and should not be interpreted as presenting the official policies or position, either expressed or implied, of the U.S. Army Research Laboratory or the U.S. Government unless so designated by other authorized documents. Citation of manufacturer's or trade names does not constitute an official endorsement or approval of the use thereof. The U.S. Government is authorized to reproduce and distribute reprints for Government purposes notwithstanding any copyright notation hereon.

REFERENCES

1. Michael B. Zellner, Gerard T. Chaney, Chester A. Benjamin, Ronald Cantrell, Robert W. Borys, Robin D. Strickland, Joshua M. Sturgill, James A. Perrella, Gerald L. Schafer, Corey E. Yonce, Martin L. Potter, Stephen Alleyne, and John M. Zajicek, *Considerations for the Design of a Multi-Color High-Speed X-ray Computed Tomography Diagnostic* ARL-TR-6969 (June 2014)
2. Moser, S.; Nau, S.; Manfred, S.; Klaus, T. In Situ Flash X-ray High-Speed Computed Tomography for the Quantitative Analysis of Highly Dynamic Processes. Meas. Sci. Technol. 2014, 25 025009.
3. Schlomka, J. P.; Roessl, E.; Dorscheid, R.; Dill, S.; Martens, G.; Istel, T.; Baumer, C.; Herrmann, C.; Steadman, R; Zeitler, G.; Livne, A.; Proksa, R. Experimental Feasibility of Multi-Energy Photon-Counting K-Edge Imaging In Pre-Clinical Computed Tomography. Phys. Med. Biol. 2008, 53 4031–4047.
4. Michael B Zellner, Charles L Randow, Ronald Cantrell, and Corey E Yonce, *Blast-Loading Assessment of Multi-Energy Flash Computed Tomography (MEFCT) Diagnostic* ARL-TR-7741 (August 2016).
5. https://www.nist.gov/pml/X-ray-mass-attenuation-coefficients, accessed August 2017.
6. Kyle Champley, *Livermore Tomography Tools (LTT) Technical Manual* LLNL-SM-687016 (March 2016)